Determination of reference concavity

The Swiss fluvial river network was delineated in ArcGIS from a 25-m-resolution digital elevation model (provided by Swisstopo). Values of k_{sn} were calculated in MatLab by performing power-law regressions on the slope-area relationships (Wobus et al., 2006) for Swiss streams. We first analyzed 132 individual stream segments from 40 watersheds throughout the Swiss Alps in order to determine a valid reference concavity. Both glacially impacted and non-glacial streams show similar slope-area relationships and yield similar concavities, with the difference that glacially impacted streams have much higher steepnesses (main text, Fig. 2a). The calculated concavities vary considerably from approximately -1 to 3, with a mean of 0.72 ± 0.65 (Fig. DR1a, b) which we apply as the reference concavity for the Swiss streams. We note that this value is higher than the 0.45 used by Korup (2006). We avoided additional potential biases related to high concavities in cirque basins by excluding all drainage areas <10 km^2 from our analyses. Lake segments were also removed. In addition, we

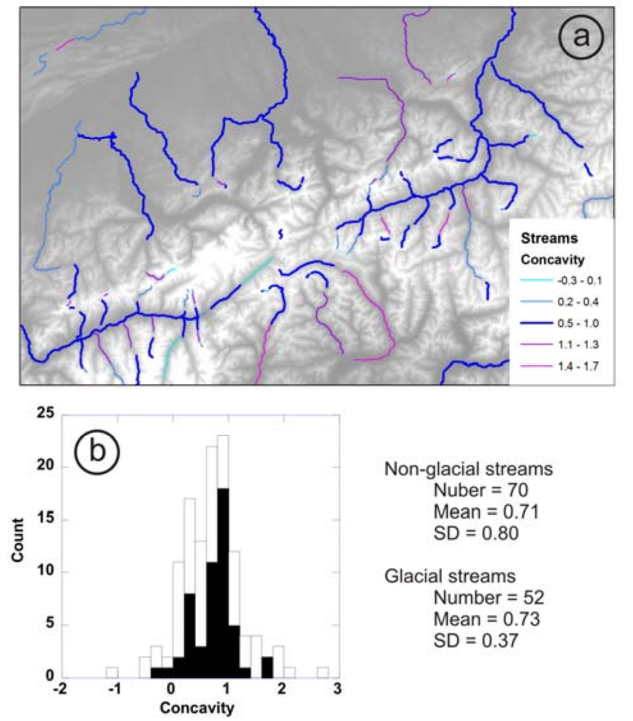

Figure DR1. a) Map view of the central Swiss Alps showing calculated stream concavities using the slope-area method. b) Histogram of concavities for both glacial (black bars) and non-glacial streams (open bars).

apply a 10 km^2 threshold contributing area, a smoothing window of 250 m, and a contour interval of 12.192m (Wobus et al., 2006).

The validity of the reference concavity approach in this varied terrain was checked by calculating the concavities of the glacially impacted basins separately from the remaining streams. The resulting concavities are nearly identical, 0.73 ± 0.37 for glacial basins and 0.71 ± 0.80 for the remaining streams (Fig. DR1b). In order to make our data comparable to existing datasets (Korup, 2006; Ouimet et al., 2009; Safran et al., 2005; Whipple, 2004; Wobus et al., 2006), we have also calculated the entire dataset using a reference concavity index of 0.45 (Figs. DR2 and DR3). The spatial density of oversteepened reaches (Figs. DR2 and main text 4a), distribution of the data (Figs. DR3c and main text 2b) and relation to lithology (Figs. DR3a and b and main text 3b and c) are similar regardless of the choice of reference concavity, with the distribution being shifted by ~1000x for θ = 0.72 vs. 0.45.

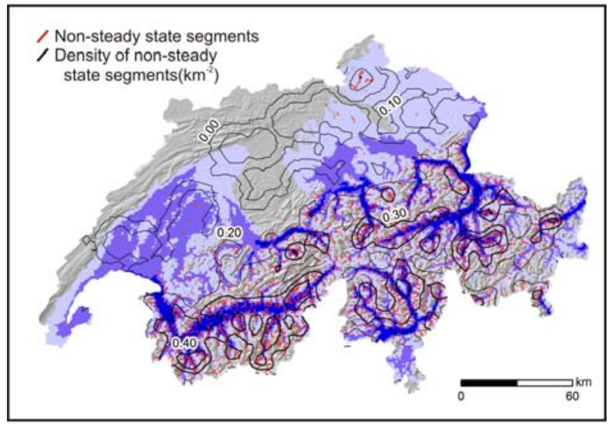

Figure DR2. Spatial distribution and density (km^{-2}) of non-steady state (oversteepened) segments using a reference concavity of 0.45 and a best-fit k_{sn} of 82 ± 40 in relation to thickness of LGM ice (darker blues indicate thicker ice). Note that the highest densities are within the Rhone and Rhine valleys.

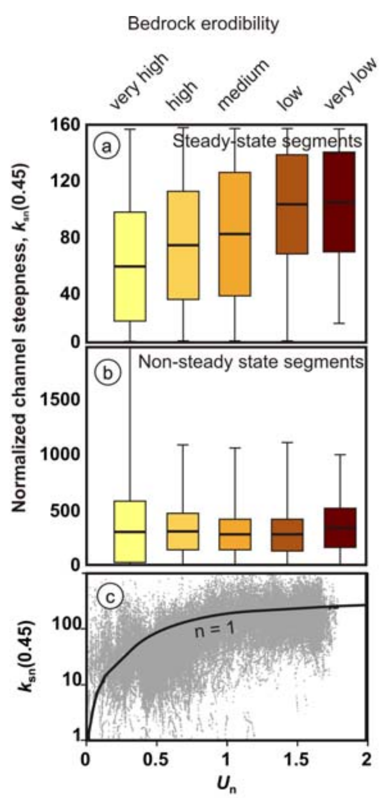

Figure DR3. a,b) pattern of k_{sn} using a reference concavity of 0.45 for different erodibility classes for steady-state and non-steady state streams, respectively. c) k_{sn} vs U_n (θ=0.45).

As a further test, we calculated the reference slope, $S_r = S*(A_r/A)^{-m/n}$ for each stream segment (Sklar and Dietrich, 1998) as this metric does not require the definition of a regional reference concavity (Wobus et al., 2006). As S_r is strongly dependent on drainage basin area, we performed the analysis for only basins between 50 and 100 km^2 using the maximum drainage basin area 33191 km^2 as the reference basin area, A_r. The resulting reference slopes exhibit the same pattern as is seen with k_{sn} (Figs. DR2, main text 4a), with the highest values and density in the Rhone and Rhine valleys (Fig. DR4).

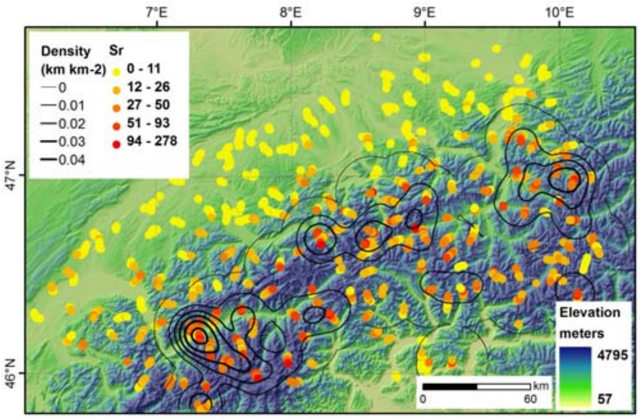

Figure DR4. Spatial density of reference slopes for 50-100km^2 drainage basins.

Modelling k_{sn} vs. U_n

The resulting k_{sn} values for $\theta = 0.72$ were then compared with vertical rock uplift rates. The uplift rates were interpolated from a data set of relative vertical movements (Schlatter et al., 2005) by universal kriging with 2nd order trend removal and 90% local weight, and exported to a 250 m resolution grid. We note that the relationship between k_{sn} and rock uplift can be fit using either linear or non-linear models and that for high values of k_{sn}, n = 2 or larger can be expected (Ouimet et al., 2009). We performed linear regressions on the log-transformed distribution using a reference concavity of 0.72 with the equation (Figs. DR3c and main text 2b):

$$\log(k_{sn}) = 1/n*\log(U_n) + \log(1/K)$$

The resulting fits were then transformed back into linear coordinates and used to model the equation:

$$k_{sn} = 1/K*U_n^{(1/n)}$$

The Alpine dataset is best described with n =1, which also gives the most conservative estimates for non-steady state reaches. We therefore model the steady-state relationship between k_{sn} and rock uplift using n = 1 (main text Fig. 2b).

Since the measured rock uplift rates are not absolute values, and because we are interested in the quantitative distribution only, we normalized the relative rates where $U_n = U + 0.446$ mm yr^{-1} to avoid negative uplift rates. The standard deviation of the steady-state model was calculated from values below the mean, in the non-skewed portion of the k_{sn}/U_n distribution (main text Fig. 2b). Values above 2 sigma of the modelled steady-state distribution are considered non-steady state values. The density map of these non-steady state river segments (Fig. 4a) was calculated using a sliding window with a radius of 20 km and is reported in km/km^2. The k_{sn} values for each bedrock erodibility class were determined for both the steady-state and the non-steady state reaches for each erodibility category. We adopted the erodibility classifications of Kühni and Pfiffner (2001) which are based on the Swiss Geotechnical Map (Niggli and de Quervain, 1936). Recently, these categories were verified by Korup and Schlunegger (2009) who measured rock strength, joint spacing and orientation, bedding and foliation orientation and degree of weathering, in order to calculate the Geological Strength Index (GSI) and geomorphic rock-mass strength (RMS).

REFERENCES

Korup, O., 2006, Rock-slope failure and the river long profile: Geology, v. 34, p. 45-48.

Korup, O., and Schlunegger, F., 2009, Rock-type control on erosion-induced uplift, eastern Swiss Alps: Earth and Planetary Science Letters, v. 278, p. 278-285.

Kühni, A., and Pfiffner, O.A., 2001, The relief of the Swiss Alps and adjacent areas and its relation to lithology and structure: topographic analysis from a 250-m DEM: Geomorphology, v. 41, p. 285-307.

Niggli P and de Quervain FD (1936) Geotechnische Karte der Schweiz. Schweizerische Geotechnische Kommission, Kümmerly and Frey, Geotechnischer Verlag, Bern.

Ouimet, W.B., Whipple, K.X., and Granger, D.E., 2009, Beyond threshold hillslopes: Channel adjustment to base-level fall in tectonically active mountain ranges: Geology, v. 37, p. 579-582.

Safran, E.B., Bierman, P.R., Aalto, R., Dunne, T., Whipple, K.X., and Caffee, M., 2005, Erosion rates driven by channel network incision in the Bolivian Andes: Earth Surface Processes and Landforms, v. 30, p. 1007-1024.

Schlatter, A., Schneider, D., Geiger, A., and Kahle, H.G., 2005, Recent vertical movements from precise levelling in the vicinity of the city of Basel, Switzerland: International Journal of Earth Sciences, v. 94, p. 507-514.

Sklar, L.S., and Dietrich, W.E., 1998, River longitudinal profiles and bedrock incision models: stream power and the influence of sediment supply, *in* Tinkler, K., and Wohl, E.E., eds., Rivers Over Rock: Fluvial Proceses in Bedrock Channels, Volume Geophysical Monograph Series, 107: Washington, DC, American Geophysical Union.

Whipple, K.X., 2004, Bedrock rivers and the geomorphology of active orogens: Annual Review of Earth and Planetary Sciences, v. 32, p. 151-185.

Wobus, C., Whipple, K.X., Kirby, E., Snyder, E., Johnson, J., Spyropolou, K., Crosby, B., and Sheehan, D., 2006, Tectonics from topography: Procedures, promise, and pitfalls, *in* Willett, S.D., Hovius, N., Brandon, M.T., and Fisher, D.M., eds., Tectonics, Climate, and Landscape Evolution: Geological Society of America Special Paper 398, Penrose Conference Series, Geological Society of America, p. 55-74.